

EXPERIMENTAL-THEORETICAL STUDY OF THE PENETRATION OF RIGID PROJECTILES AND IDENTIFICATION OF SOIL PROPERTIES

V. G. Bazhenov, A. M. Bragov, and V. L. Kotov

UDC 539.3 : 620.17.254

The parameters of the Grigoryan soil model are determined using an experimental-computational method previously proposed and the results of reversed experiments on penetration of projectiles with flat and hemispherical heads at impact velocities of 50–450 m/sec in sandy soil. It is shown that the quasistationary dependences of the resistance force on impact velocity obtained in the reversed experiment can be used to solve problems of deep penetration of projectile in soil with an error not exceeding the measurement error.

Key words: *soil, mathematical modeling, experiment, penetration, identification.*

Penetration. The impact and penetration of projectiles in soil have been studied extensively (see, for example, [1–16]). However, these studies were primarily concerned with the penetration of rigid projectiles in plastic (clay and loamy) soils [8–16]. In [13, 14], an experimental-theoretical method of dynamic penetration was proposed to determine the shear resistance of clay soil as an ideally plastic medium with the Tresca–Saint Venant plasticity condition; this approach was elaborated in [15–17]. Using the hypotheses of incompressibility and ideal plasticity and other simplified concepts of dynamic soil behavior, which are valid to some extent for plastic soil, domestic [1–4, 17–25] and [5, 6, 26–31] foreign authors have developed analytical methods for studying the penetration of rigid bodies of revolution into soil.

There have been a few experiments investigating the pulsed loading of loose soil [31–33], and the properties of these media are less understood. In experimental studies [34–36] of the dynamic compressibility of sandy soils with a plane shock wave, only the shock adiabat of the medium was determined. The compressibility of the medium in penetration experiments was also determined in [37]. The use of a modified Kolsky method [38, 39] with a system of split Hopkinson bar to study the compressibility and plastic properties of soil is restricted by the elastic limit of the material of the measuring bar and holders, which does not exceed 0.5 GPa. Thus, at present, effective methods for studying physicomaterial properties of soil over a wide range of pressure have been developed insufficiently.

It seems promising to extend the experimental-computation approach of [40] to study soil properties under dynamic loading using well-known soil models [41, 42], methods of mathematical modeling of impact and penetration of deformable projectiles in soil [42–47], and data of reversed experiments [10, 11]. The dependence of the penetration resistance on the parameters of the soft soil model has been studied previously. It has been established that features of the time dependence of the resistance force allow the force maximum to be used to determine the dynamic compressibility of soil [37], and the quasistationary value can be used to determine its strength (elastoplastic) characteristics [48, 49]. A convergent iterative process has been constructed to refine current values of material functions in a sample by minimizing the objective function using a series of computational experiments.

In the present work, dynamic compressibility parameters and the pressure dependence of the yield point are determined using an experimental-computational method [40] and the results of reversed experiments on penetration in sandy soil projectiles with flat and hemispherical heads at impact velocities 50–450 m/sec.

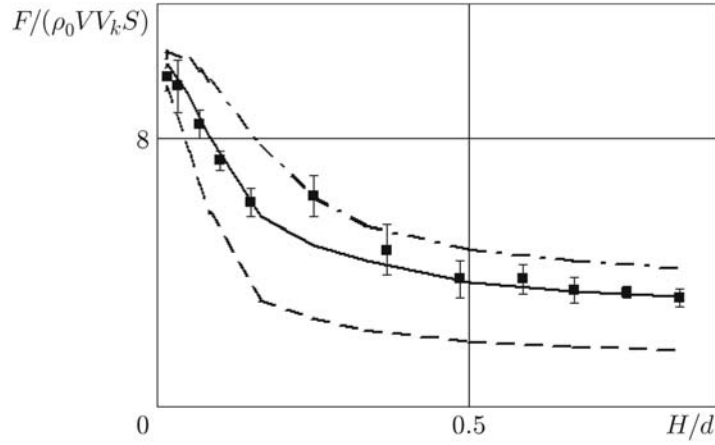


Fig. 1. Resistance to penetration a flat-nosed projectile in sandy soil versus penetration depth: points correspond to experiments, curves to calculations (solid curves correspond to calculations using the obtained parameters of the model, dot-and-dashed curves to calculations using the pressure linear dependence of the yield point, and dashed curve to calculations in a hydrodynamic approximation).

1. Mathematical Model. The mathematical model of the dynamic deformation of shock-loaded soil is formulated in [41] using mass and pulse conservation laws and the plastic flow equations, which in cylindrical coordinates rOz (Oz is the symmetry axis) are given by the system of differential equations

$$\begin{aligned} \frac{d\rho}{dt} + \rho(u_{r,r} + u_{z,z}) &= -\frac{\rho u_r}{r}, & \frac{d\rho_*}{dt} &= \frac{d\rho}{dt} h(\rho - \rho_*) h\left(\frac{d\rho}{dt}\right), \\ \rho \frac{du_r}{dt} - \sigma_{rr,r} - \sigma_{rz,z} &= \frac{\sigma_{rr} - \sigma_{\theta\theta}}{r}, & \rho \frac{du_z}{dt} - \sigma_{rz,r} - \sigma_{zz,z} &= \frac{\sigma_{rz}}{r}, \\ D_J s_{ij} + \lambda s_{ij} &= 2G e_{ij} \quad (i, j = r, z) \end{aligned}$$

and the finite relations

$$p = f_1(\rho, \rho_*) h(\rho_* - \rho) h(\rho_0 - \rho), \quad s_{ij} s^{ij} = 2\sigma_y^2/3, \quad \sigma_y \equiv f_2(p).$$

Here h is a Heaviside function, t is time, ρ_0 , ρ , and ρ_* are the initial, current, and maximum densities reached during loading, u_i , σ_{ij} , s_{ij} , and e_{ij} are the components of the velocity, Cauchy stress tensor, and stress tensor and strain rate deviators, respectively, p is the pressure, D_J is Jaumann's derivative, d/dt is the total time derivative, G is the shear modulus, σ_y is the yield point. The parameter $\lambda = 0$ in the case of elastic strain, and $\lambda > 0$ if the Mises–Schleicher plasticity condition is satisfied, the symbol after comma denotes differentiation with respect to the corresponding variable; the summation is performed over repeated indices; the unknown functions f_1 , f_2 are to be determined.

The parameters of the equation of state for soil are determined from the results of reversed experiments using a measuring bar [10, 11] and numerical modeling of the impact and penetration of cylindrical bars in soil. The reversed experiment is performed as follows [47]. A container filled with soil is accelerated to the required velocity and impacts the motionless head a projectile fixed on a measuring bar. The impact velocity and the properties of the bar material should be such that no plastic deformations arise in the bar. In this case, the impact gives rise to an elastic strain pulse $\varepsilon(t)$ in the bar. By recording this pulse in the measuring bar, it is possible to determine the force F acting on the projectile during its interaction with the medium from the known relation $F(t) = E\varepsilon(t)S$, where E is the elastic modulus of the bar and S is the cross-sectional area. Thus, in the experiment, the force measurement reduces to recording the elastic strain pulse in the bar, which greatly simplifies this experiment due to strain measurements.

Figure 1 shows curves of the resistance to penetration of a flat-nosed projectile in sand versus penetration depth in the reversed experiment. The values of the resistance force and penetration depth are normalized to $\rho_0 V V_k S$ and d ($V = 335$ m/sec is the velocity of projectile penetration in sand, $V_k = 120$ m/sec is the sound velocity in sand, $S = \pi d^2/4$ is the midsection area of the projectile, and d is the diameter of the projectile cross section). The sandy soil was a dry mixture of quartz sand of natural composition. The range of dispersion of experimental data are plotted from the results of six experiments with a confidence probability of 0.95. The experimental data are given for $H/d < 1$ because the shock compressibility can be determined given only the maximum value of the force [11] whereas determination of the shear characteristics of soil requires the quasistationary value of the resistance force.

In [48, 49], the following procedure for identifying the plastic properties of soil was proposed. The initial data are experimental dependences of quasistationary values of the resistance to penetration of a flat-nosed projectile on initial impact velocity. The required pressure dependence of the yield point is determined by minimization (which does not require additional conditions) of the functional describing the total difference between theoretical

and experimental data in a certain range of velocities: $\sum_{i=1}^N |F_i - F_i^*|/|F_i^*| \rightarrow \min$ (F_i^* and F_i are experimental and calculated quasistationary values of the resistance to penetration with initial velocity V_i).

For approximate solution of the formulated optimization problem, the pressure dependence of the yield point is written in discrete form $\sigma_y(p) \equiv \sigma_y^{i-1} + \alpha^i(p - p^{i-1})$ ($p^{i-1} \leq p < p^i$, where $i = \overline{1, N}$). The discretization nodes were determined so as to satisfy the condition $|F_i - F_i^*|/F_i^* < \delta$, where δ is a specified small quantity. For this, in the numerical calculation for impact velocities $V_i > V_{i-1}$, the tangent α_i of the i th segment of the broken line is adjusted until the calculated and experimental values of the quasistationary resistance force coincide. The reference pressure values p of the piecewise linear function $\sigma_y(p)$ are determined as the average pressure on the impacted end of the bar in the numerical solution of the problem.

2. Results of Numerical Calculations. An example of the practical implementation of the identification procedure proposed in [48, 49] is the determination of the plasticity function in a dry sandy mixture with an initial density $\rho_0 = 1.72$ g/cm³. The shock adiabat for this soil was determined in reversed experiments [37] at impact velocities $V = 50$ – 450 m/sec, and it is close to the linear dependence of the shock-wave velocity D on the mass velocity u behind the wavefront $D = A + bu$ ($A = 455$ m/sec and $b = 2.3$). In experiments [34] with a plane shock wave for a sandy mixture, close values were obtained for $A = 500$ m/sec and $b = 2.41$.

Numerical calculations were performed in an axisymmetric setting. The determining relations between the bulk strain $\varepsilon = 1 - \rho_0/\rho$ and the soil pressure p were obtained using the dependence $f_1 \equiv M\varepsilon^n$ (M and n are constants) [33] at $p = 0.01$ – 1.00 MPa, the dependence $f_1 \equiv \rho_0 a^2 \varepsilon / (1 - b\varepsilon)^2$ [34–36] at $p > 150$ MPa, and an interpolating cubic polynomial [46, 47, 50] at $p = 1$ – 150 MPa. Bulk unloading of soils is approximated with sufficient accuracy for practical applications by the linear pressure–density relation determined by the tangent to the shock adiabat at a certain limiting (hydrodynamic) point $\rho_\infty = 2.5$ g/cm³; the shear modulus is proportional to the unloading modulus [42, 51].

On the projectile head in contact with the soil medium, nonpenetration conditions along the normal and frictional sliding in the tangential direction were imposed. Because the soil flow around the cylindrical part adjoining the end has a separation (cavitation) nature, the normal and shear stresses on the free surfaces of the soil and projectile were set equal to zero. The outer boundaries of the calculation region of the soil were considered rigid and corresponding to the geometry of the holder used in the reversed experiment. The soil region was partitioned by a difference grid into square cells with side sizes R/m (R is the radius of the cylindrical part of the projectile and m is the number of cells). The convergence of the employed modified Godunov method [52, 53] was analyzed in a series of numerical calculations on refined grids. The quasistationary dependence of the resistance on the cell size R/m is nearly linear with a confidence not less than 0.95, and the difference between the forces obtained for $m = 80$ and the forces predicted for $m = \infty$ does not exceed 3%.

Figure 2 shows the dimensionless dependence of the resistance to penetration of a flat-nosed projectile in sand in the quasistationary stage versus projectile velocity. The data presented in Fig. 2 were obtained for impact velocities $V = 48, 100, 180, 275,$ and 335 m/sec and averaged over five experiments. The confidence probability is 0.95.

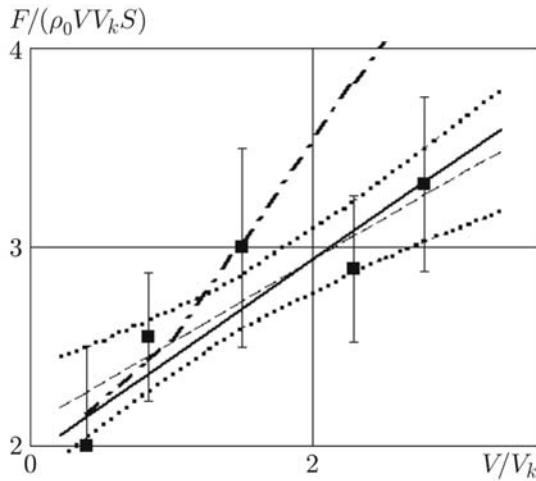


Fig. 2

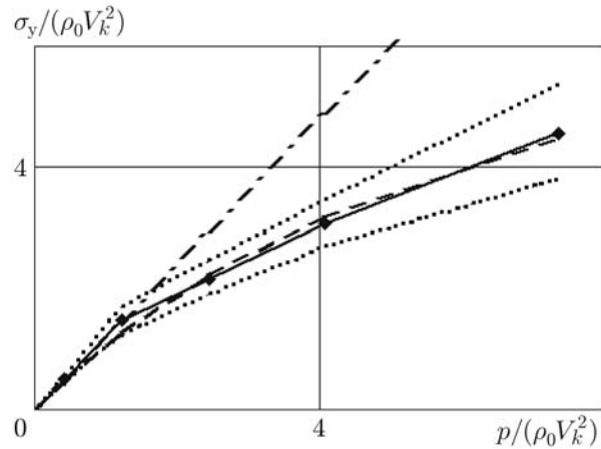


Fig. 3

Fig. 2. Quasistationary resistance to penetration of a flat-nosed projectile in sandy soil versus impact velocity: points correspond to experiments, curves to calculations (solid curve corresponds to calculations using the obtained parameters of the model, and the dot-and-dash curve to calculations using the linear pressure dependence of the yield point); the dashed curve is the regression line, and the dotted curve is the boundary of the error corridor.

Fig. 3. Yield point it versus pressure in sandy soil at various impact velocities: points correspond to experiments, curves to calculations (the dashed curve corresponds to the nonlinear dependence $f_2 \equiv \sigma_0 + \mu p / (1 + \mu p / \sigma_{\max})$, the solid curve to the two-link approximation, the dash-and-dotted curve to the linear dependence $f_2 \equiv \mu p$); and the dotted curves to the boundaries of the error corridor.

Figure 3 shows the pressure dependence of the yield point on in sand soil calculated using the procedure of [48, 49] for the same impact velocities. It is evident that an increase in the pressure leads to a decrease in the growth rate of the yield point, which is due to the grinding of soil particles upon impact and penetration. In addition, with increasing pressure, the contribution of the shear components to the solution decreases and the calculation error of the dependence of the shear resistance on projectile velocity increases.

The discrete pressure dependence of the yield point shown in Fig. 3 is approximated by a nonlinear dependence of the form $f_2 \equiv \sigma_0 + \mu p / (1 + \mu p / \sigma_{\max})$ [42] with constants $\sigma_0 = 0.01$ MPa, $\mu = 1.14$, and $\sigma_{\max} = 275$ MPa, but, in view of the errors, it can also be approximated by a two-link broken line and the linear dependence $f_2 \equiv \mu p$ which was used as the initial approximation.

The results of calculations using the linear pressure dependence of the yield point are in good agreement with experimental data only for impact velocities below 200 m/sec. The results of numerical modeling using the nonlinear dependence of the yield point obtained by identification are in the error corridor.

Figure 4 shows dimensionless curves of the resistance to penetration of a projectile with a hemispherical head with an initial velocity of 250 m/sec in sand versus penetration depth and impact velocity. The midsection area of the hemispherical projectile was determined taking into account flow separation: $S = \pi(\sin \varphi d)^2 / 4$ and $\varphi = \pi / 3$ [1, 2]. The confidence intervals were constructed by four experiments with a confidence of 0.95.

Figure 5 gives Lagrangian difference grids obtained by numerical calculations of penetration of cylindrical projectiles with flat and hemispherical head in soil. At the initial time (before impact), the undeformed uniform grid consisted of square cells. Deformation of the grid indicates that condensed and partially ground soil is attached to the heads of the projectiles and move together with the projectiles [1, 13, 32]. The size of the condensed region depends on flow characteristics. The maximum attached mass is formed near the flat end. Penetration of the projectile with a hemispherical head is accompanied by separation of soil particles from the contact surface at a flow separation angle approximately equal to 60° [1, 2]. The cylindrical part of the projectile which bounds the contact surface and its midsection is shown in Fig. 5b by dashed curves. For the projectile shapes considered, the quasistationary resistances normalized to the midsection area of the contact surface differ only slightly, which

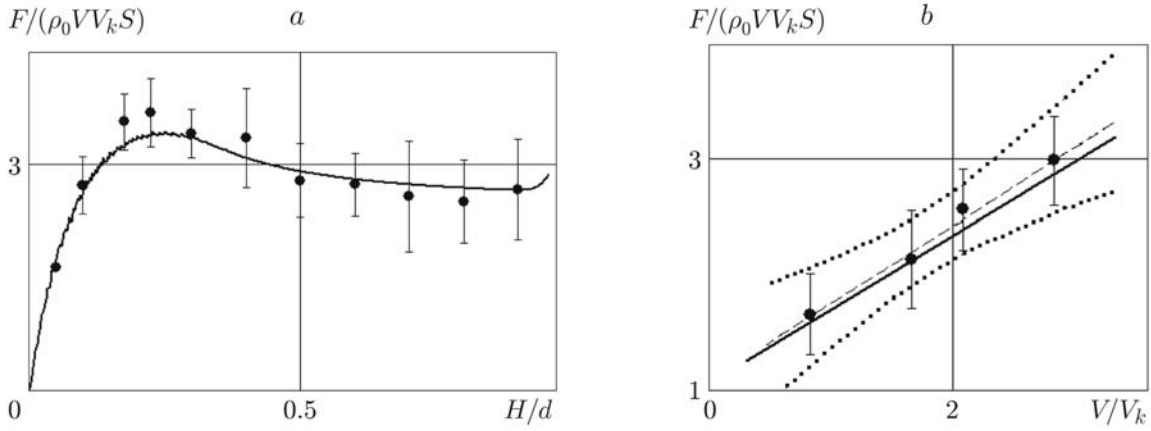


Fig. 4. Resistance to penetration of projectile with a hemispherical head in sandy soil versus penetration depth (a) and impact velocity (b): points correspond to experiments, solid curves to calculations, the dashed curve is the regression line, and the dotted curves are the boundaries of the error corridor.

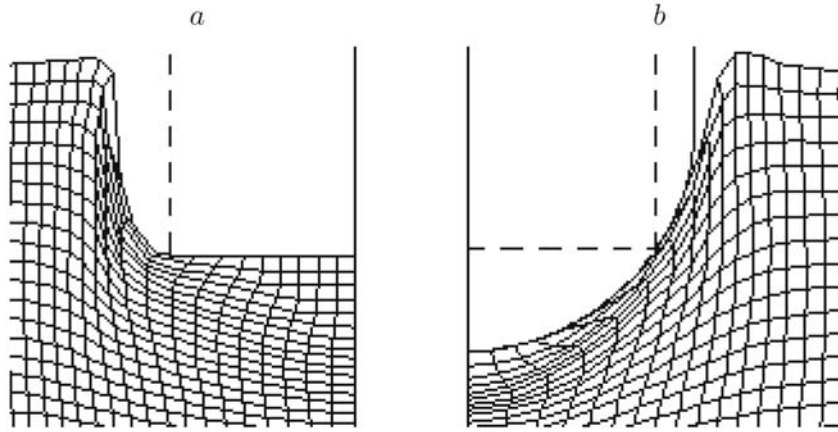


Fig. 5. Fragments of Lagrangian difference grids obtained in numerical calculations of penetration of cylindrical projectiles with flat (a) and hemispherical (b) heads in sandy soil: dashed curves show the cylindrical part of the projectile.

supports the hypothesis [23] of similarity between flow processes in the developed stage of penetration of blunted bodies in soft soils.

Below, we consider the applicability of the results of reversed experiments to the determination of the penetration depth of bodies of finite mass. In direct experiments [31], values were obtained for the coefficients of the quadratic dependence of the acceleration of a moving body on the penetration velocity $-dV/dt = \alpha V^2 + \beta V + \gamma$. For $\gamma = 0$, the Resal penetration formula is obtained, and for $\beta = 0$, the Poncelet penetration law. These dependences of the penetration depth on the penetration velocity $H(V)$ are written as

$$H(V) = H_k + \frac{1}{\alpha} \ln \left(\frac{\beta + \alpha V}{\beta + \alpha V_k} \right); \quad (1)$$

$$H(V) = H_k + \frac{1}{2\alpha} \ln \left(\frac{\gamma + \alpha V^2}{\gamma + \alpha V_k^2} \right). \quad (2)$$

Formulas for the maximum penetration depths at initial velocity V are obtained from Eqs. (1) and (2) for $H_k = V_k = 0$. In [31], it is proposed to use the Poncelet law (2) at velocities lower than a certain critical value V_k and the dependence $-dV/dt = \alpha V^2$ at $V > V_k$. In addition, there are theoretical and experimental data [12, 23, 31] indicating different nature of projectile penetration in the supersonic, transonic, and subsonic modes.

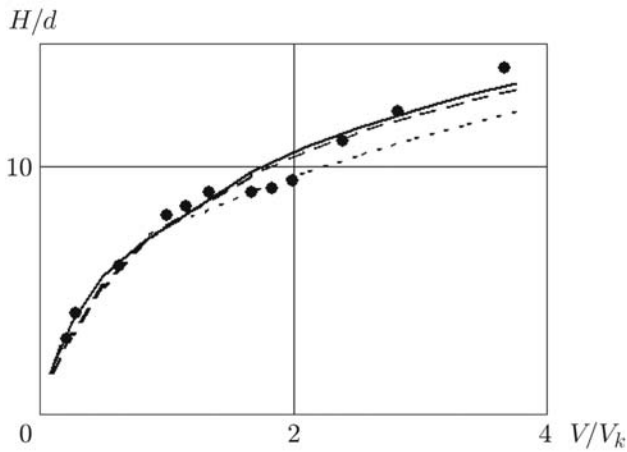


Fig. 6

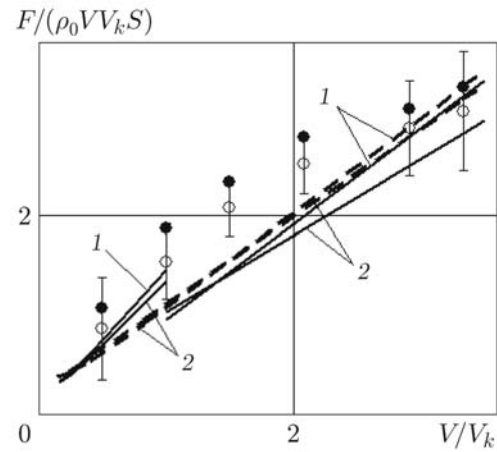


Fig. 7

Fig. 6. Penetration depth of projectile with a hemispherical head in sandy soil versus penetration velocity: points correspond to the experiment of [12, 32], solid curves to the experiment of [31], dashed curve to the approximation of the results of [12, 32] by the Resal formula, and the dashed curve to the calculation performed in the present work.

Fig. 7. Resistance to penetration of a projectile with flat head (filled points) and hemispherical head (open points) in sandy soil versus penetration velocity: 1) experiment of [31]; 2) experiment of [32]; solid curves correspond to the approximation of the resistance according to the penetration law with a discontinuity at $V_k = 120$ m/sec proposed in [31], dashed curves to the continuous approximation by the Resal formula; points correspond to the calculation performed in the present work; the errors of reversed experiments are shown by the intervals.

Using approximations of the form (1) or (2) for the dependence of the penetration depth on penetration velocity of a sphere in sandy soil (points in Fig. 6) obtained in direct experiments, it is possible to find the resistance penetration as was done in [14, 31]. Figure 7 gives dependences of the penetration resistance on penetration velocity normalized to the quantity $\rho_0 V V_k S$ (for a flat-nosed cylinder with the midsection, area of the wetted surface is $S = \pi d^2/4$, and for a spherical projectile, area of the wetted surface is $S = 0.75\pi d^2/4$). The error of the results of the reversed experiment was 15–20%.

We note that in [31] the depth of penetration of cylinders of diameter d in quartz sand with grain size $d_1 \approx d/13$ was recorded by a photoelectric chronograph. The coefficients α , β , and γ in (1) and (2) were determined from data on the time dependence of the position of the projectiles [31]. Dependences of the penetration depth of a steel sphere of diameter d in sandy soil with particle size $d_1 \leq d/15$ on the initial impact velocity were obtained in [32].

In Fig. 7, it is evident that, in view of flow separation for spherical projectiles (flow separation angle $\varphi = \pi/3$), the results of experiments obtained in various settings for sand with different grain size are fairly close. The cause of this is that, due to the intense grinding of particles of the medium in the supersonic penetration mode, the fractional composition of the soil becomes almost identical.

The obtained dimensionless dependences of the resistance on penetration velocity (see Fig. 7) were used to estimate the penetration depth of a spherical projectile in a half-space occupied by sandy soil.

Figure 8 gives curves of the penetration resistance versus velocity for penetration of a projectile with a hemispherical head in sandy soil with a constant velocity and by inertia for various initial impact velocities. In each calculation, the resistance force increases from zero to the maximum value with its subsequent decrease to the value predicted by the results of reversed experiments. The duration of the nonstationary stage of penetration is inversely proportional to the mass of the projectile and is directly proportional to the cross-sectional area of the projectile; in the calculation of the depth of penetration of a massive body normally to the free surface, the nonstationary stage can be ignored.

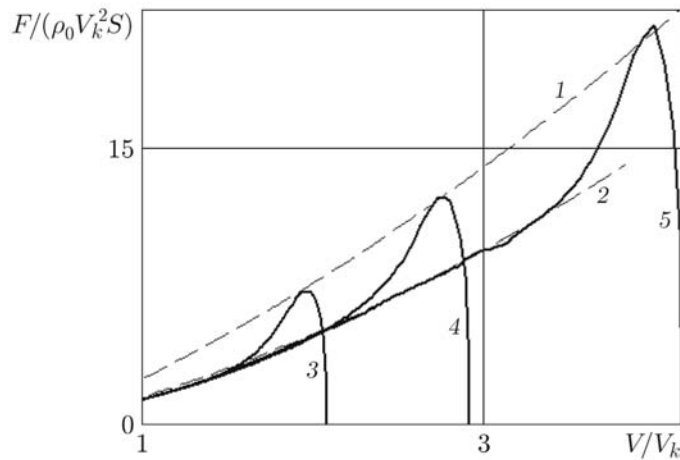


Fig. 8. Penetration resistance of a projectile with a hemispherical head in sandy soil versus penetration velocity: dashed curves refer to constant velocity (curve 1 refers to maximum resistance and curve 2 refers to quasistationary resistance) and solid curves correspond to an initial velocity of $V = 250$ (3), 350 (4), and 500 m/sec (5).

Conclusions. The parameters of the dependences of the pressure on density and yield point in dry sandy soil were determined using the experimental-theoretical method of identifying the parameters of the equation of state for soft soil proposed in [40] and the results of reversed experiments on penetration of projectiles with flat and hemispherical heads in sandy soil. Good agreement between the calculation and experimental data at impact velocities of 50–450 m/sec confirms the efficiency of the method developed in [48, 49] in the velocity and pressure ranges in which the shear properties of soil are of significance.

The analysis of available experimental data and numerical-calculation results on penetration of projectiles of various shapes in sandy soil shows that the penetration parameters at supersonic velocities are determined primarily by the shear strength of the medium and depend weakly on the initial fractional composition.

The data of the reversed experiments cited in the paper were obtained by V. V. Balandin and A. M. Bragov.

This work was supported by Council on Grants of the President of the Russian Federation for Support of Leading Scientific Schools of the Russian Federation (Grant No. NSh-3367.2008.8), Young Russian Scientists (Grant No. MK-4839.2008.8), and the Russian Foundation for Basic Research (Grant Nos. 08-01-00500-p and 08-08-00883-p).

REFERENCES

1. Kh. A. Rakhmatullin, A. Ya. Sagomonyan, and N. A. Alekseev, *Problems of Soil Dynamics* [in Russian], Izd. Mosk. Gos. Univ., Moscow (1964).
2. A. Ya. Sagomonyan, *Penetration* [in Russian], Izd. Mosk. Gos. Univ., Moscow (1974).
3. V. N. Aptukov, *Applied Theory of Penetration* [in Russian], Nauka, Moscow (1992).
4. V. M. Fomin, A. I. Gulidov, G. A. Sapozhnikov, et al., *High-Velocity Interaction of Bodies* [in Russian], Izd. Sib. Otd. Ross. Akad. Nauk, Novosibirsk (1999).
5. M. E. Backman and W. Goldsmith, "The mechanics of penetration of projectiles into targets," *Int. J. Eng. Sci.*, **16**, No. 1, 1–99 (1978).
6. W. Goldsmith, "Non-ideal projectiles impact on targets," *Int. J. Impact Eng.*, **22**, No. 1, 95–395 (1999).
7. A. G. Gorshkov and D. V. Tarlavovskii, *Impact on Soil: Mechanics of Contact Interactions* [in Russian], Fizmatlit, Moscow (2001), pp. 409–416.
8. Yu. K. Bivin, V. V. Viktorov, and L. P. Stepanov, "Motion of a solid in clay," *Izv. Akad. Nauk SSSR, Mekh. Tverd. Tela*, No. 2, 159–165 (1978).

9. Yu. N. Bukharev, V. P. Gandurin, A. E. Korablev, et al., "Experimental study of the penetration of a rigid projectile in a clay medium and snow," in: *Applied Problems of Strength and Plasticity: An Analysis and Optimization of Structures* [in Russian], Nizhny Novgorod State University, Novgorod (1991), pp. 99–106.
10. G. E. Hauver, "Penetration with instrumented rods," *Int. J. Eng. Sci.*, **16**, No. 11, 871–877 (1978).
11. B. V. Balandin and A. M. Bragov, "Experimental technique for measuring resistance forces during interaction of a projectile with soil," in: *Applied Problems of Strength and Plasticity: Methods of Solution* [in Russian], Nizhny Novgorod State University, Novgorod (1991), pp. 101–104.
12. Yu. K. Bivin, "Motion of a solid in a perturbed medium," *Izv. Ross. Akad. Nauk, Mekh. Tverd. Tela*, No. 5, 91–98 (2002).
13. Yu. K. Bivin, V. V. Viktorov, and B. Ya. Kovalenko, "Determination of the dynamic characteristics of soils using a penetration method," *Izv. Akad. Nauk SSSR, Mekh. Tverd. Tela*, No. 3, 105–110 (1980).
14. Yu. K. Bivin, V. A. Kolesnikov, and L. M. Flitman, "Determination of the mechanical properties of media using a dynamic penetration method," *Izv. Akad. Nauk SSSR, Mekh. Tverd. Tela*, No. 3, 181–185 (1982).
15. I. K. Kokhanenko, S. F. Maklakov, and V. A. Prishchepa, "Determination of the shear strength of soil under dynamic loading," *Izv. Akad. Nauk SSSR, Mekh. Tverd. Tela*, No. 4, 182–184 (1990).
16. Yu. N. Bukharev, A. E. Korablev, and M. I. Khaimovich, "Experimental determination of shear stress on the projectile surface during dynamic penetration in soil," *Izv. Ross. Akad. Nauk, Mekh. Tverd. Tela*, No. 2, 186–188 (1995).
17. D. B. Balashov and N. V. Zvolinskii, "Flow of an elastoplastic medium past a cone," *Izv. Ross. Akad. Nauk, Mekh. Tverd. Tela*, No. 3, 46–53 (1996).
18. L. Ya. Lyubin and A. S. Povitzkii, "Oblique impact of a solid on soils," *J. Appl. Mech. Tech. Phys.*, No. 1, 55–60 (1966).
19. F. M. Borodich, "Dynamic interaction of blunted axisymmetric solids on soil," *Prikl. Mekh.*, **24**, No. 11, 117–121 (1988).
20. L. M. Flitman, "High-velocity nonseparation elastoplastic flow around a blunted body," *Prikl. Mat. Mekh.*, **54**, No. 4, 642–651 (1990).
21. A. G. Akopyan, "Penetration of a rigid cone into a plastically orthotropic half-space," *J. Appl. Mech. Tech. Phys.*, No. 5, 159–163 (1991).
22. D. A. Demen'shin and S. V. Krylov, "Numerical modeling of normal penetration of solids in porous soils," in: *Applied Problems of Strength and Plasticity: Numerical Modeling of Physicomechanical Processes*, Nizhny Novgorod State University, Nizhny Novgorod (1991), pp. 103–106.
23. S. S. Grigoryan, "Approximate solution of the problem of penetration of a body in soil," *Izv. Ross. Akad. Nauk, Mekh. Zhidk. Gaza*, No. 4, 18–24 (1993).
24. V. A. Kolesnikov, "Calculation of the trajectory and estimation of the dimensions of the strain localization zone during penetration of a sphere in soil," *Izv. Ross. Akad. Nauk, Mekh. Tverd. Tela*, No. 2, 59–64 (1997).
25. K. Yu. Osipenko and I. V. Simonov, "Supersonic flow of a porous medium around a cone," *Izv. Ross. Akad. Nauk, Mekh. Tverd. Tela*, No. 2, 87–96 (2001).
26. M. J. Forrestal, D. B. Longcope, F. R. Norwood, et al., "A model to estimate forces on conical penetrators into dry porous rock," *Trans. ASME, J. Appl. Mech.*, **48**, No. 3, 25–29 (1981).
27. X. W. Chen and Q. M. Li, "Deep penetration of a non-deformable projectile with different geometrical characteristics," *Int. J. Impact Eng.*, **27**, 619–637 (2002).
28. T. L. Warren, S. J. Hanchak, and K. L. Poormon, "Penetration of limestone targets by head-nosed VAR 4340 steel projectiles at oblique angles: Experiments and simulations," *Int. J. Impact Eng.*, **30**, 1307–1331 (2004).
29. D. Durban and R. Masri, "Conical indentation of strain-hardening solids," *Europ. J. Mech., A: Solids*, **27**, 210–221 (2008).
30. Z. Rosenberg and E. Dekel, "A numerical study of the cavity expansion process and quantity application to long-rod penetration mechanics," *Int. J. Impact Eng.*, **35**, 147–154 (2008).
31. W. Allen, E. Mayfield, and H. Morrison, "Dynamics of a projectile penetrating sand," *J. Appl. Phys.*, **28**, 370 (1957).
32. Yu. K. Bivin, "Penetration of solids in loose and layered media," *Izv. Ross. Akad. Nauk, Mekh. Tverd. Tela*, No. 1, 154–160 (2008).
33. G. V. Rykov, "Experimental study of the stress field during explosion in sandy soil," *J. Appl. Mech. Tech. Phys.*, No. 1, 85–89 (1964).

34. V. A. Lagunov and V. A. Stepanov, "Measurement of dynamic compressibility of sand at high pressures," *J. Appl. Mech. Tech. Phys.*, No. 1, 88–96 (1963).
35. M. Dianov, N. A. Zlatin, S. M. Mochalov, et al., "Shock compressibility of dry and water-saturated sand," *Pis'ma Zh. Tekh. Nauk*, **2**, No. 12, 529–532 (1976).
36. A. M. Bragov and G. M. Grushevskii, "Effect of the humidity and grain size on the shock compressibility of sand," *Pis'ma Zh. Tekh. Nauk*, **19**, No. 12, 70–72 (1993).
37. A. M. Bragov, V. V. Balandin, A. K. Lomunov, and A. R. Filippov, "Determination of the shock adiabat of soft soils from the results of reversed experiments," *Pis'ma Zh. Tekh. Nauk*, **32**, No. 11, 52–55 (2006).
38. A. M. Bragov, G. M. Grushevsky, and A. K. Lomunov, "Use of the Kolsky method for confined tests of soft soils," *Exp. Mech.*, **36**, No. 3, 237–242 (1996).
39. A. M. Bragov, V. L. Kotov, A. K. Lomunov, and I. V. Sergeichev, "Measurement of the dynamic characteristics of soft soils using the Kolsky method," *J. Appl. Mech. Tech. Phys.*, **45**, No. 4, 580–585 (2004).
40. V. G. Bazhenov "Mathematical modeling and methods of identification of the deformation and strength characteristics of materials," *Fiz. Mezomekh.*, **10**, No. 5, 91–105 (2007).
41. S. S. Grigoryan, "Main concepts of soil dynamics," *Prikl. Mat. Mekh.*, No. 4, 1057–1072 (1960).
42. B. V. Zamyshlyayev, *Models of Dynamic Deformation and Failure of Soil Media* [in Russian], Nauka, Moscow (1990).
43. V. I. Kondaurov, I. B. Petrov, and A. S. Kholodov, "Numerical modeling of the process of penetration of a rigid body of revolution into an elastoplastic barrier," *J. Appl. Mech. Tech. Phys.*, No. 4, 625–632 (1984).
44. G. A. Kirilenko and A. Ya. Sagomonyan, "Numerical modeling of penetration in a soil," *Izv. Akad. Nauk ArmSSR, Mekhanika*, **39**, No. 1, 47–51 (1986).
45. S. M. Bakhrakh, O. A. Vinokurov, G. V. Gorbenko, et al., "Numerical investigation of the process of nondeformable cylinder penetration at constant velocity into a compressible fluid," *J. Appl. Mech. Tech. Phys.*, No. 5, 815–810 (1989).
46. V. G. Bazhenov, A. M. Bragov, V. L. Kotov, and A. V. Kochetkov, "Investigation of the impact and penetration of solids of revolution in a soft soil," *Prikl. Mat. Mekh.*, **67**, No. 4, 686–697 (2003).
47. V. G. Bazhenov, V. L. Kotov, S. V. Krylov, et al., "Experimental-theoretical analysis of nonstationary interaction of deformable impactors with soil," *J. Appl. Mech. Tech. Phys.*, **42**, No. 6, 1083–1089 (2001).
48. V. G. Bazhenov, V. L. Kotov "Identification of the dynamic compressibility and shear resistance of soil during penetration of projectiles," *Dokl. Ross. Akad. Nauk*, **408**, No. 3, 333–336 (2006).
49. V. G. Bazhenov and V. L. Kotov, "Method of identification of the elastoplastic properties of soils during penetration of projectiles," *Izv. Ross. Akad. Nauk, Mekh. Tverd. Tela*, No. 4, 184–190 (2008).
50. V. G. Bazhenov, V. L. Kotov, A. V. Kochetkov, et al., "Numerical modeling of loading of sandy soil by explosion of a pressure charge," *Izv. Ross. Akad. Nauk, Mekh. Tverd. Tela*, No. 2, 70–77 (2001).
51. V. L. Kotov, "Application of the Grigoryan model to problems of dynamic deformation of sandy soil," in: *Problems of Strength and Plasticity* (collected scientific papers) [in Russian], No. 66, Nizhny Novgorod State University, Nzhny Novgorod (2004), pp. 123–127.
52. V. G. Bazhenov, E. A. Kozlov, and S. V. Krylov, "Numerical modeling of nonlinear two-dimensional problems of shock interaction of deformable media and structures using the Godunov method," in: *Applied Problems of Strength and Plasticity: Investigation and Optimization of Structures* (collected scientific papers), Gor'kii Univ., Gor'kii (1990), pp. 99–106.
53. V. G. Bazhenov and V. L. Kotov, "Modification of Godunov's numerical scheme for solving problems of pulsed loading of soft soils," *J. Appl. Mech. Tech. Phys.*, **43**, No. 4, 603–611 (2002).